Water Masses in the Gulf of Aden

MOHAMMED ALI AL SAAFANI[1]* and S. SATHEESH CHANDRA SHENOI[2]

[1]*Department of Earth Science and Environment, Faculty of Science, Sana'a University, Sana'a, Yemen*
[2]*National Institute of Oceanography, Goa - 403 004, India*

Hydrographic data collected from Gulf of Aden since 1920 have been compiled to identify and refine the definitions of water masses in the Gulf of Aden (GA) and to describe their spatio-temporal variability. Four water masses have been identified based on their θ-S characteristics. The Red Sea Water (RSW) that flows from the Red Sea is the most prominent water in the GA; this occupies about 37% of the total volume of Gulf of Aden. The Gulf of Aden Surface Water (~3%) forms as a mixture of local water and the water from western Arabian Sea during winter and Red Sea surface water during summer. The intermediate water, identified as Gulf of Aden Intermediate Water (GAIW), occupies about 9% of the total volume of GA; a characteristic salinity minimum is associated with it at $\sigma_\theta = 26.50$ kg m^{-3}. The northward spread of sub-tropical subsurface water from the south appears to be the major source of GAIW. The bottom water, named Gulf of Aden Bottom Water, showed the least variability. It was formed due to the mixing of Red Sea Water and water of southern origin. Mixing triangles have been used to analyze the composition of water in the GA.

1. Introduction

The Gulf of Aden (GA), a narrow strip of water that connects the Red Sea with the Indian Ocean, extends east-northeastward from the narrow Strait of Bab-el-Mandab to a line connecting Ras Baghashwa (east of Mukalla, Yemen) and Ras Asir (northern corner of the Somali Peninsula). The 900 km long GA spreads over an area of about 220×10^3 km^2. The average depth is about 1800 m. A hot dry climate prevails over the landmasses surrounding the GA, though the prevailing winds have a pronounced seasonal cycle. Strong westerly winds blow during the summer monsoon (June–August) and weak northeasterly winds blow during the winter monsoon (November–February). During intermediate periods (April–May and October), winds are weak and unstable in their directions.

From an oceanographic perspective, the GA is important because it provides the passage for Red Sea Water (RSW), one of the most saline water masses in the world oceans, into the Indian Ocean. It is also significant

commercially, because it is an important highway for international trade between the east and the west. In spite of its importance, very little information is available on its hydrography and biological productivity. A few studies have used the available hydrographic data to describe the water masses in the GA. Rochford (1964) identified two water masses in the eastern GA, namely, high salinity Arabian Sea Water (ASW at σ_t levels 23.5–24.0) and RSW (at σ_t levels 27.0–27.4). Khimitsa (1968) identified four layers of water in the GA based on their physical and chemical properties. A top layer (50–100 m) of high salinity (36.0–36.5 psu) and high oxygen content, an intermediate layer, between 100–500 m, of lower salinity (~35.3 psu) and low oxygen content, another intermediate layer, between 500–1000 m, of high salinity RSW (~36.5–38.0 psu), and a layer near the bottom containing the bottom water of low salinity (~34.9–35.5 psu) and temperature. He suggested that the water in the upper intermediate level enters the Gulf from the south as a strong jet between Cape Gvardafui and Socotra at depths ~150 to 200 m. He noted that the Southern Ocean is the origin of the bottom water. Piechura and Sobaih (1986) described three water masses in the upper 1000 m of GA. They named them Surface Water, Subsurface Water, and RSW. They suggested that local heating and evaporation are the causative factors for the formation of surface water, which

---

* Corresponding author. E-mail: alsafany@nio.org
  Present address: National Institute of Oceanography, Goa - 403 004, India.

is deeper in winter (200–300 m) and shallower in summer (70–80 m). For the subsurface water the highest temperature and salinity were found in winter. They suggested a subtropical front as the origin of Subsurface Water. Nasser (1992) also identified three water masses in the upper 1000 m of the northern Gulf of Aden, namely: Surface High Salinity water, Subsurface Low Salinity water and RSW. He concluded that the Subsurface Low Salinity Water is transported in the GA from the Somali basin during the summer monsoon. More recently, Mohamed et al. (1996) and Mohammed (1997) identified four salinity maxima in the GA. They identified the first maximum between the σ_t levels 24.0 and 25.0, the second between 25.0 and 26.0, the third between 26.0 and 27.0 and the fourth between 27.0 and 28.0. They identified the third maximum as a mixture of waters originating from the Persian Gulf, Timor Sea and Subtropical Subsurface and the fourth maximum as a mixture of Red Sea water, Antarctic Intermediate water and Timor Sea water. Most of the other studies of the GA (Maillard and Soliman, 1986; Fedorov and Meshchanov, 1988; Bower et al., 2000) dealt only with the outflow and spreading of RSW. Ozgokman et al. (2003), Peter and Johns (2005) and Peter et al. (2005) described the structure and dynamics of Red Sea outflow plume in the western GA.

All these studies were either localized in space or time or focused on Red Sea outflow. None of them provide a comprehensive picture of the structure of water masses in the GA as they evolve round the year nor provide a quantitative estimate. Furthermore, the temperature-salinity-σ_θ range of the water masses defined by various authors often varied drastically depending on the limited data they had used for their studies. In this study, temperature-salinity climatology has been used to define the θ-S-σ_θ range of water masses rather than the limited data used in previous studies. For this purpose, we used a new temperature-salinity climatology created using all available temperature-salinity profiles from this region. Based on well demarcated boundaries of the water masses, we have also calculated the volumes occupied by the water masses and their changes throughout the year. Data and methodology are described in Section 2. Section 3 describes the results based on vertical and horizontal structure of water masses and Section 4 presents discussions and conclusions.

2. Data and Methodology

A new hydrographic dataset was assembled using temperature-salinity profiles from (i) the archives of National Oceanographic Data Center (NODC); (ii) Japan Oceanographic Data Center (JODC); (iii) the CTD profiles collected during the Bab-el-Mandab Experiment (Murray and Johns, 1997; Al Saafani and Shenoi, 2004); (iv) the CTD profiles available from the Netherlands In-
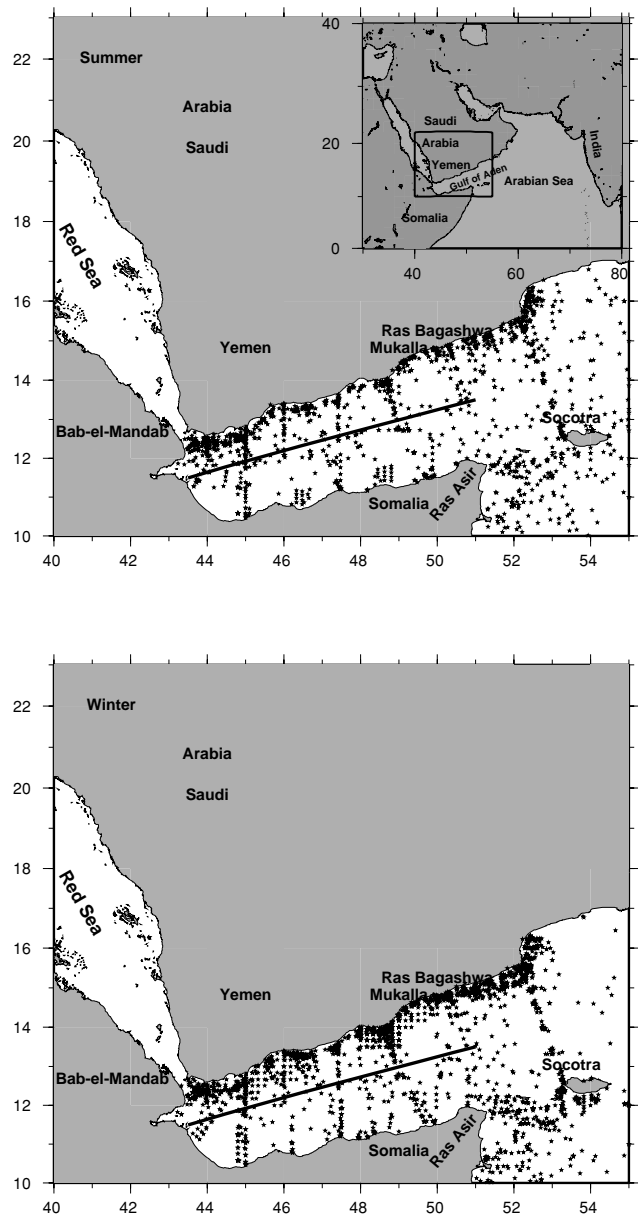

Fig. 1. Area map of Gulf of Aden and distribution of the location of temperature-salinity profiles used to identify the water masses. 4088 T-S profiles were used; among them 2641 also contained oxygen data. The distribution of data is shown separately for (a) summer (1705 θ-S profiles) and (b) winter (2383 θ-S profiles). The line along the axis of the Gulf represents the east-west axis of GA (approximately). Sections shown in Figs. 6 and 10 pertain to this line.

dian Ocean Programme (Baars, 1994); and (v) the data collected during 1984–85 by Marine Science and Resources Research Center, Yemen (Stirn et al., 1985). A total of 23144 temperature and 6514 salinity profiles were obtained from these sources. Before proceeding further,
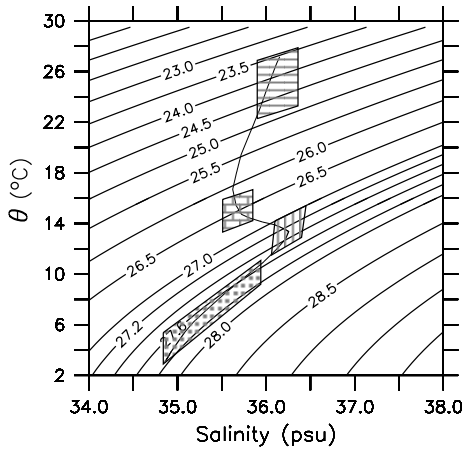
Fig. 2. Typical θ-S curve for GA. Four water masses are identified from the profiles.

2102 duplicate profiles were identified and isolated. The temperature-salinity values in the west are very different from those in the east. Hence, to assess the quality of the profiles, the monthly means and standard deviations were computed at each depth level separately in 2° longitude × 2° latitude bins. Values (temperature or salinity) exceeding more than three standard deviations were then removed. The profiles that passed this check were then examined for large inversions in temperature and stability following Boyer and Levitus (1994). Of 4412 temperature-salinity profiles, 4088 profiles met the stated quality criteria. Among them, 2541 profiles also contained data on oxygen. The distribution of stations (Fig. 1) is uneven, but not alarming. The number of temperature-salinity profiles is always higher near the coast of Yemen. The earlier climatology included only 13229 temperature profiles (Boyer *et al.*, 2002) and 1917 salinity profiles (Stephens *et al.*, 2002) for this region bounded between 43.5°E and 55.0°E. Hence, we expect improvements in the robustness of the new climatology.

A typical θ-S curve for the GA (Fig. 2) clearly shows four distinct water masses similar to those reported by Khimitsa (1968). The upper three water masses also show similarities to those reported by Piechura and Sobaih (1986) and Nasser (1992). Mohamed *et al.* (1996) reported five water masses in the GA, but the temperature-salinity-density ranges they used to define the water masses varied drastically from ours. The θ-S curve in Fig. 2 shows high saline surface water followed with low saline water in the intermediate levels and high saline water below that. The bottom water is comparatively fresher than that in the upper water column. Such θ-S curves constructed individually and collectively were then used for further analysis.

To compute the volume of each water mass, we have adopted the method proposed by Montgomery (1958). Due to the paucity of data, the volume computations were done for seasons rather than for months. Similarly, due to the paucity of data in some of the 1° × 1° grids, the volume computations were carried out over a 1° longitude band. A mean θ-S curve for 1° longitude band was computed first and then sliced in to 0.5°C temperature × 0.1 psu salinity grids (see Fig. 7). The volume of each grid was then estimated by multiplying their respective thicknesses by the surface area of a 1° longitude band. The volumes of 0.5°C temperature × 0.1 psu salinity grids falling within the pre-defined bounds of the water masses (based on θ-S-σ_θ ranges) were then added together to determine the total volume of water mass.

3. Results

3.1 T-S characteristics

Figure 3 shows the θ-S diagrams constructed using temperature-salinity profiles available from the GA west of 51°E. The number of profiles available during a month varied from 146 in December to 313 in January. About 40% of the profiles extended only up to 400 m. Since GA receives high saline Red Sea water in the west and moderately saline Arabian Sea water in the east, we have divided the region in to three sub-regions, namely: the western region (between 43.5°E and 45.0°E), the central region (between 45.0°E and 49.0°E), and the eastern region (between 49.0°E and 51.0°E).

Four water masses are identifiable from the θ-S diagrams in Fig. 3. They are: (i) a salinity maxima near the surface between the σ_θ levels 22.20 kg m^{-3} and 24.80 kg m^{-3}; we call this water Gulf of Aden Surface Water (GASW); Khimitsa (1968) called it Surface Aden Water. (ii) A salinity minimum between the σ_θ levels 26.20 and 26.90 kg m^{-3}; we call this water Gulf of Aden Intermediate Water (GAIW); Khimitsa (1968) called it Low Salinity Layer or subsurface salinity minimum. (iii) A salinity maximum between the σ_θ levels 26.90 and 27.50, which is easily identifiable as Red Sea Water (RSW). Finally, (iv) a distinct water between the σ_θ levels 27.50 and 27.80; we call this Gulf of Aden Bottom Water (GABW); Khimitsa (1968) called this Bottom Water. Among the four water masses, the θ-S relationship is tightest for the bottom water mass, but the potential temperature and salinity varies over a wider rage (3 to 9°C and 34.70 to 35.60 psu). The ranges of potential temperature and salinity for the four water masses are given in Table 1. The histograms (Fig. 4) show the distribution of potential temperature and salinity within the four water masses. Histograms are useful for the identification of core potential temperature and salinity. For example, the potential temperature and salinity of the GASW core is 25.5°C and 36.0 psu. Similarly, the potential temperature and salinity of the
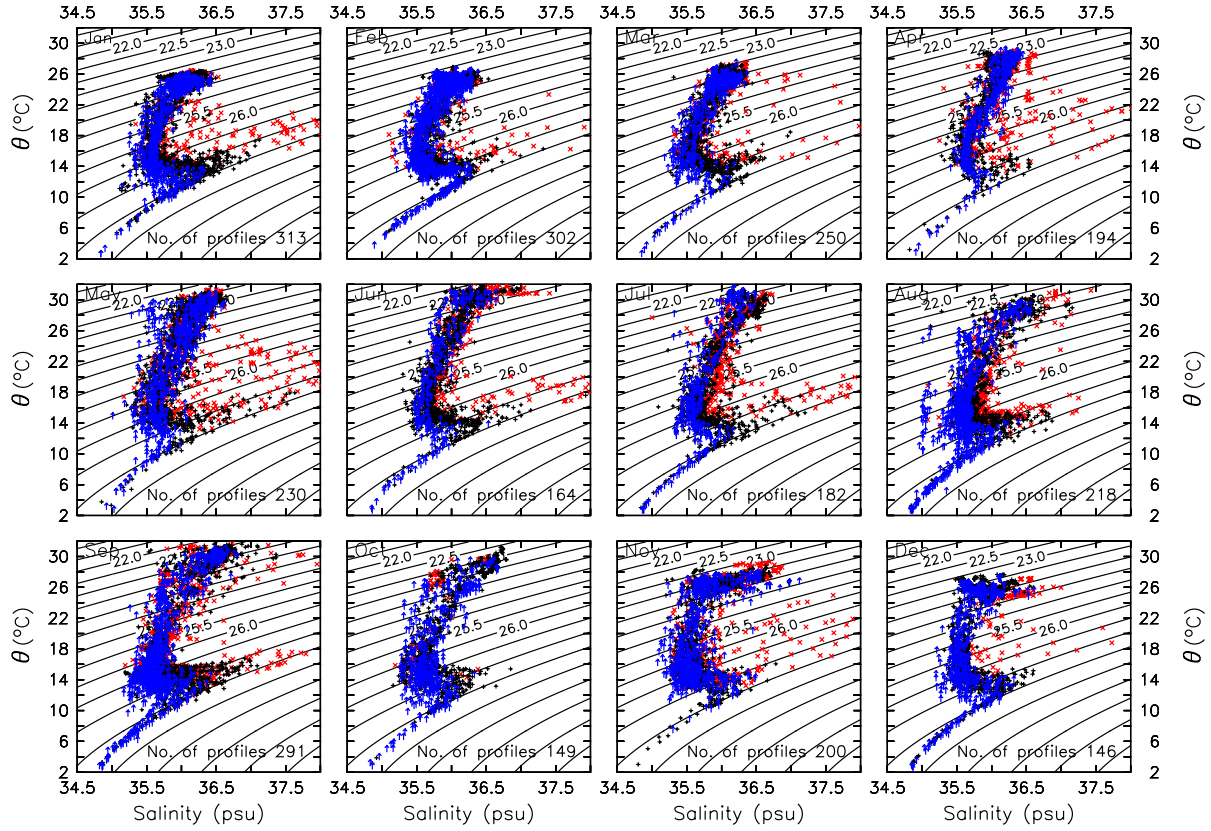
Fig. 3. θ-S diagram for GA for all months. All available profiles from the GA (west of 51°E) are included. Profiles from the region west of 45°E are in red (western region), those in the region between 45–49°E are in black (central region) and those from the region between 49°E and 51°E are in blue (eastern region). Number of θ-S profiles available during each month is also indicated.

Table 1. Potential temperature-salinity-σ_θ and depth ranges of the water masses in the GA.

Water mass	θ (°C)	S (psu)	σ_θ (kg m^{-3})	Depth (m)
GASW	21.0–32.0	35.4–36.8	22.20–24.80	0–100
GAIW	12.0–17.0	35.1–36.4	26.20–26.90	120–420
RSW	7.0–20.0	35.2–38.2	26.90–27.50	350–1050
GABW	3.0–9.0	34.7–35.6	27.50–27.80	1200–1600

RSW core is 12.5°C and 35.8 psu respectively.

Gulf of Aden Surface Water:

The spatio-temporal variability of the salinity of the GASW that occupies the surface layer is not more than 1.00 psu (Fig. 3), but the potential temperature ranges between 21.0°C and 32.0°C during summer and 22.0°C and 26.0°C during winter. The cooler surface temperature during winter is due to the cool dry northeasterlies that blow over the northern Arabian Sea and adjoining areas (Piechura and Sobaih, 1986). Accordingly, the lower limit of its σ_θ range also undergoes wide variations from 23.50 kg m^{-3} in January–February to 22.20 kg m^{-3} in June–July. GASW is seen in all three regions of the gulf: western, central and eastern. The profile-to-profile variation in salinity is at a maximum in the western region and a minimum in the central one. Few profiles in the western region showed salinities as high as 37.00 psu during August–September due to high saline surface water outflow from the Red Sea during summer. Similarly, a few profiles in the eastern region showed lower salinities (35.5 psu) than expected (Fig. 3). Since the profiles observed over several years are included for this analysis, inter-annual variability is also a reason for the large variations.
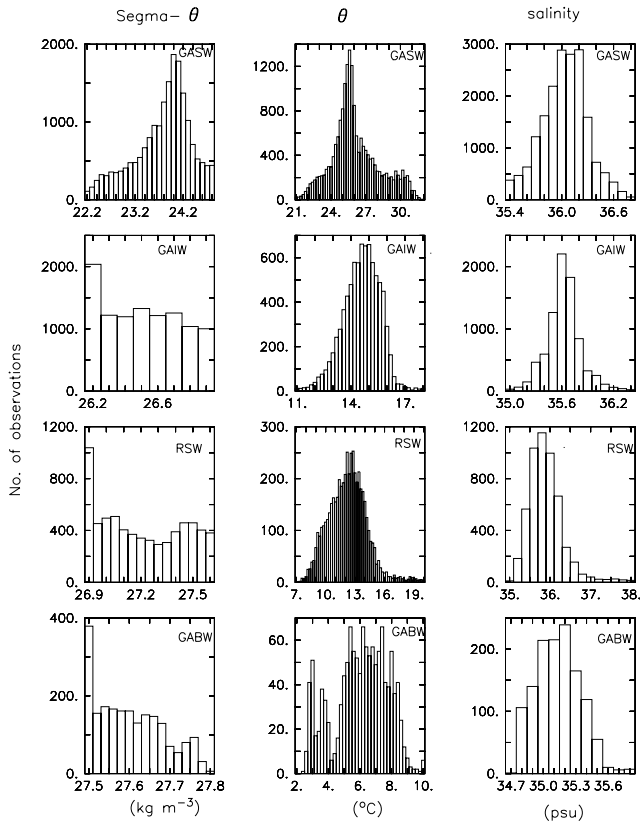
Fig. 4. Histograms of potential density, potential temperature and salinity for GASW, GAIW, RSW and GABW. The histograms were constructed by counting the data values constrained within the θ-S-σ_θ ranges given in Table 1.

Gulf of Aden Intermediate Water:

This water, identifiable by a salinity minimum, showed very little variability from month to month compared to GASW (Fig. 3). Its core, situated at σ_θ level 26.50, is well defined throughout the year. On average, the spatio-temporal variability in the range of salinity and potential temperature is less than 0.75 psu and 3.0°C. The salinity in the eastern region is comparatively lower than that in the central one. The salinity profiles in the western region showed large variations (>2 psu). Some of them must have occurred due to the high salinity water that outflows from Bab-el-Mandab into the GA (Maillard and Soliman, 1986; Murray and Johns, 1997; Al Saafani and Shenoi, 2004).

Red Sea Water:

This is the most prominent water mass in the GA and there is no ambiguity about its origin. It outflows into the GA from the Red Sea through Bab-el-Mandab strait; its core exists at σ_θ level 27.20. 68% of the observations showed salinities in the range 35.30 to 36.00 psu and 32% of them showed salinity greater than 36.00 psu. The pro-

files from the western region show salinities as high as 38.00 psu (see Fig. 3 for January and May–July). In the central region, both potential temperature and salinity showed large variability, especially during the summer months (May–September). The outflow of RSW from the Red Sea undergoes a seasonal cycle in response to the monsoon winds (Murray and Johns, 1997); the outflow is minimum at the end of the summer monsoon season and maximum during the peak of winter. Hence, in addition to the inter-annual variability, the seasonal variability in the θ-S could well be associated with the variability in the outflow of RSW from the Red Sea.

Gulf of Aden Bottom Water:

The GABW is easily identifiable in the σ_θ range 27.50 to 27.80. Though this water mass has a narrow σ_θ rage, its potential temperature and salinity has wider ranges; the potential temperature ranges between 3.0 and 9.0°C and salinity between 34.70 and 35.60 psu (Fig. 4). Being bottom water, the temporal variability of the θ-S structure is very low.

3.2 Horizontal distribution

The spatial distribution of θ-S profiles alone is insufficient to describe the variations in the horizontal distribution of the water masses. Hence, maps of horizontal distribution of water masses were prepared for two major seasons: the summer (August–September) and the winter (January–February). Here we chose the last two months of the seasons because the circulation effects on the water mass are best seen towards the end of the season. The salinity at the core of the water mass is used as a tracer to describe the horizontal distribution (Fig. 5). The core is defined using the maximum/minimum salinities. For example, for RSW we pick the maximum salinity between the σ_θ levels 26.90 and 27.50 and for GAIW we pick the minimum salinity between the σ_θ levels 26.20 and 26.90. As expected, the salinity of the core of RSW is higher in the west due to the discharge from the Red Sea. The core of RSW flows within the depth range 600–650 m except in few pockets where it deepens to 700–800 m. This is consistent with the description of Bower *et al.* (2000) and Bower *et al.* (2005). On average, the core of RSW shallows during summer, in the east, by about 50–100 m. The lowest salinity in the core is seen near the Somali coast at around 49.0°E in both seasons. Low salinities are also seen near the coast of Yemen in summer.

The salinity in the core of GAIW water increases towards the west. The salinity in the core is considerably higher in the west due to mixing with high saline outflow from the Red Sea (Khimitsa, 1968; Piechura and Sobaih, 1986). The core shallows by at least 50 m during summer from its winter position. From the pattern of salinity contours it appears that the GAIW spreads from east to west. The salinity distribution in the core of GASW is very dif-

ferent from that for RSW and GAIW. The core salinities are highest in the central region and lowest in the eastern region. In summer, a large patch of high salinity, exceeding 36.10 psu, occupies the central region between 45°E and 48°E. The large patch of high salinity is due to the anticyclonic eddy that forms in the GA in summer (Piechura and Sobaih, 1986).

The structure of these water masses is also clearly seen in the vertical section running through the middle of the gulf (Fig. 6). The GAIW and the GABW spread from the east while the RSW spreads from the west.

3.3 Volumetric analysis

The volumes occupied by the water masses, estimated following Montgomery (1958), for an average θ-S profile in the GA, are shown in Fig. 7. For this purpose, the average depth of GA was assumed as 2000 m. As per the estimate, the volume of RSW in the GA is about
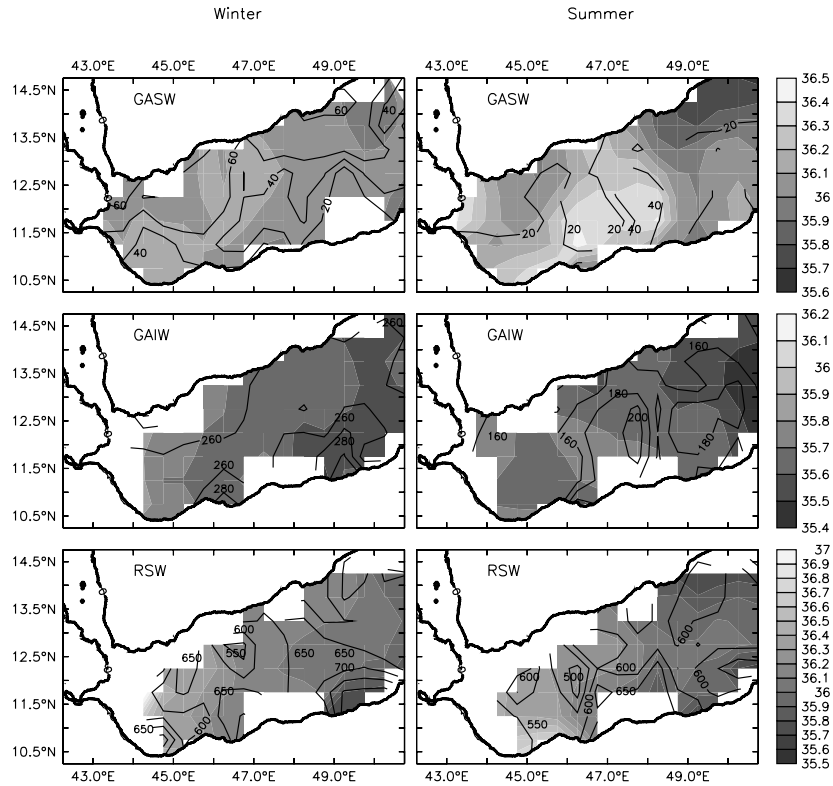

Fig. 5. Horizontal distribution of the water masses during summer (August–September) and winter (January–February). The salinity (psu) in the core layer of the water mass is used to trace the spread of the water mass. The contours represent depth of core layer.
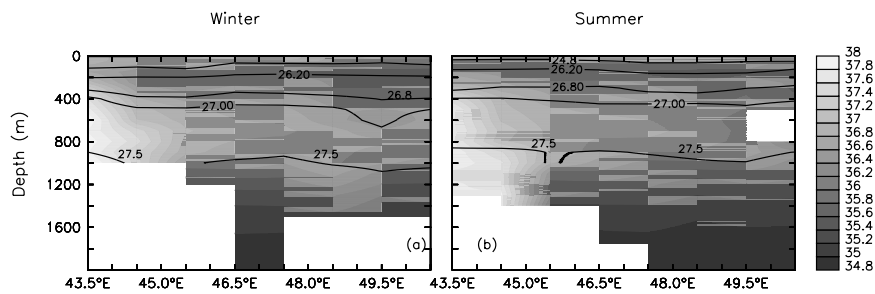

Fig. 6. Vertical section of salinity (psu) along the east-west axis of GA (see Fig. 1) (a) for winter (January–February) and (b) for summer (August–September). σ_θ contours are also shown.

1769.0×10^{11} m^3 while the volumes of GAIW and GABW are about 418.7×10^{11} m^3 and 1851.3×10^{11} m^3 respectively. The volume of GASW is only about 138.0×10^{11} m^3. In terms of percentages, the RSW occupies ~37% of the total volume of GA while GAIW and GABW occupy ~9% and 38% respectively.
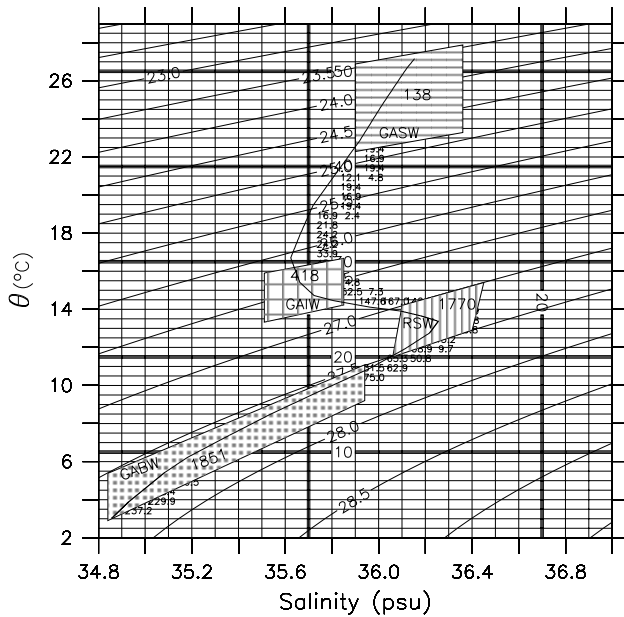
While the estimates based on the mean θ-S profile

Fig. 7. θ-S-V diagram constructed for an annual mean profile from the Gulf of Aden. The volumes ($\times 10^{11}$ m^3) occupied by GASW, GAIW, RSW and GABW are marked in different shades. Thin lines represent the 0.5°C × 0.1 psu θ-S grid. The θ-S grids used to estimate volumes of water masses are shown in different shades. The σ_θ lines are also shown. Assuming an average depth of 2000 m, the total volume of GA is ~4840×10^{11} m^3.

for the GA provided the approximate volumes of water masses, they are inadequate to describe the temporal and spatial variability. Estimates based on monthly mean θ-S profiles within 1° grids spread over the GA would have been ideal to describe the spatial and temporal variability. The data sparseness, however, prevents such estimates. Hence, mean θ-S profiles were constructed for two seasons (summer and winter) for 1° spatial grids. Since the mean θ-S profiles in several grids do not extend beyond 1200 m, it will not be possible to estimate the volume of GABW. The volumes thus estimated for 1200 m deep water column along the east-west axis of GA are shown in Fig. 8. During winter, the volume of RSW is 100×10^{11} m^3 in the western grid and it is 72×10^{11} m^3 in the eastern grid. In the center it is ~88×10^{11} m^3; the sharp decrease (~72×10^{11} m^3) occurs only in the grids east of 49°E. During summer, though the volume of RSW remains more or less the same (~100×10^{11} m^3) in the west, it decreases gradually towards the east (Fig. 8).

GAIW is present more in the east (25×10^{11} m^3) than that in the west (~12×10^{11} m^3) during winter. In summer, however, both the east-west variation and the volume are low (~18–20 $\times 10^{11}$ m^3). The volume of GASW is about 10×10^{11} m^3 in winter and about 6×10^{11} m^3 in summer. The east-west variability in the volume of GASW during both seasons is negligible.

All three water masses, the RSW, the GAIW and the GASW, had higher volumes during winter than in summer. The increase in volumes results in increased sea level during winter. The seasonal cycle of sea level recorded by satellite altimeter as well as the tide gauge at Aden show an increase of ~35 cm during winter (figure not shown).

3.4 Percentage composition of GA water

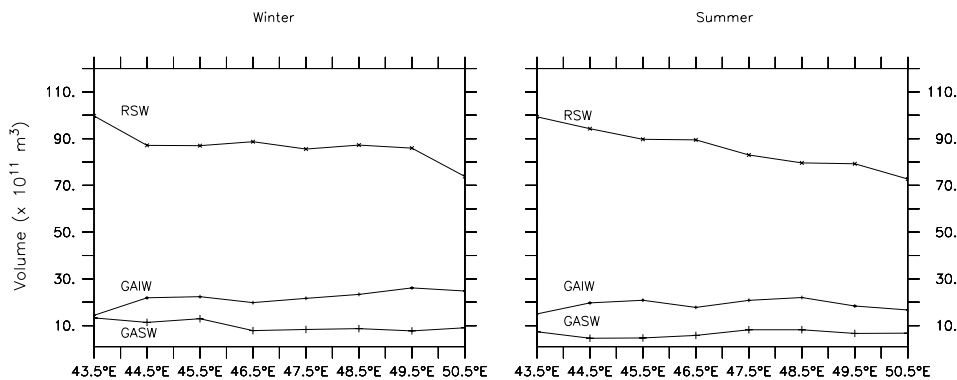The percentage composition of water masses in a water sample in the GA was estimated following Tomczak

Fig. 8. East-west variations in the volumes of water masses in the GA ($\times 10^{11}$ m^3). Meridonally (1° wide longitude bands) averaged θ-S profiles were used to estimate the volumes following the θ-S-V diagrams.

(1981a, b). The method is an extension of the mixing triangle theory. Conserving the mass, the relative contribution of any water mass to the water sample at a location can be determined from the linear system of equations given as

$$AX = B$$

where A is an $n \times n$ matrix of the parameter values for the n water masses, B is a vector of n elements which contains $n - 1$ observations, and X is a vector of n elements which gives the relative contributions of the water masses. Since four water masses are to be considered to describe the composition of water samples in the GA, three parameters were considered, namely: potential temperature, salinity and O_2. Consideration of O_2 as one of the parameters might introduce an element of uncertainty in the estimate because it is not a conservative tracer, especially in the shallow depths (depths <200–300 m). Nevertheless, we have used O_2 as one of the parameters in the absence of other suitable ones. Matrix A was defined using the thermohaline indices of the water masses before they entered and mixed in the GA (Table 2); i.e., the θ-S of the water mass when it was outside the GA. Mixing triangles were used to determine the thermohaline indi-

Table 2. Thermohaline indices for the four water masses in the GA.

Water mass	θ (℃)	Salinity (psu)	Oxygen (ml L^{-1})
GASW	27.00	36.10	5.00
GAIW	14.50	35.25	0.70
RSW	18.50	37.90	0.50
GABW	3.10	34.80	2.00

ces (see for example Fig. 9). GAIW and GABW enter the GA from the east, hence the profiles from the eastern region were used to determine their thermohaline indices. Similarly, the profiles from the western region were used to determine the thermohaline index for RSW before it entered the GA. A similar definition of thermohaline index for GASW could be ambiguous because that does not have a definite source region. Part of the GASW forms within the GA due to air-sea fluxes and part is advected into the GA either from the western Arabian Sea and/or from the Red Sea. The surface flow in the GA inferred from the climatology of sea level height anomalies estimated from the satellite altimetry is towards the west during the winter and towards the east during the summer (Al Saafani and Shenoi, 2006). Hence, the profiles from eastern (western) GA were used to determine the thermohaline index during winter (summer).

The percentage composition of water in the GA along the east-west axis (see Fig. 1) is shown in Fig. 10. As expected, the percentage of water of Red Sea origin reduces from 90% in the west (near Bab-el-Mandab) to less than 40% in the east (Figs. 10(e) and (f)). The water in the bottom (deeper than 1100 m) as well as the surface and intermediate (less than 400 m) levels also contains about 10–20% water of Red Sea origin. Similarly, the water that is responsible for the GAIW is at a maximum in the intermediate levels; it also contributes to the water that is found in the deeper layers (deeper than 1200 m) and surface levels (less than 100 m). The presence of more of this water in the east than in the west suggests that the water responsible for GAIW enters the Gulf from the east. The water that is responsible for the GASW does not contribute much to the water below 150 m. It is at a maximum (>90%) in the surface layers (<40 m), decreasing rapidly towards the deeper layers. Most of this water also appears to enter the GA from the east. The water that is
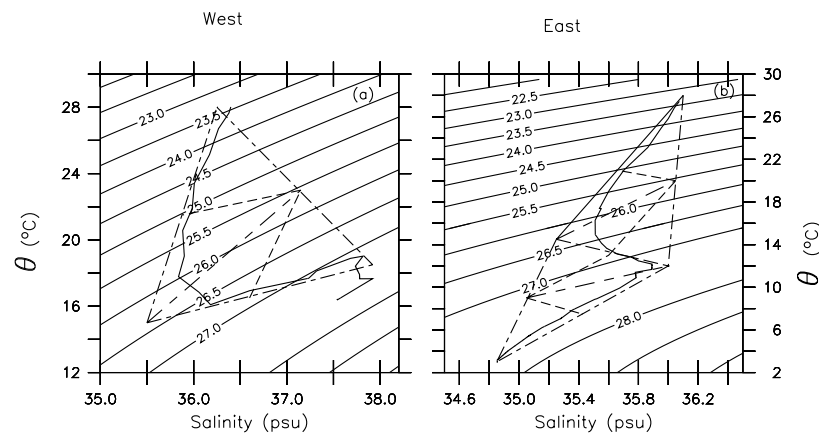

Fig. 9. Typical mixing triangles for the western and eastern GA. They were used to identify the thermohaline indices of water masses (see Table 2).

responsible for the formation of GABW shows highest concentrations (~90%) in the bottom layers and dilutes rapidly towards the upper layers (<1200 m).

4. Discussion and Conclusions

Previous reports (Khimitsa, 1968; Piechura and Sobaih, 1986; Nasser, 1992; and Mohamed *et al*., 1996) used limited data sets to describe the water mass in the GA. Though they succeeded in identifying the water masses, they failed to give an integrated picture of the presence of distinct water masses in the GA. Moreover, the definitions and nomenclature of the water masses varied, except for the RSW. In this paper, while refining the earlier work, we also present quantitative estimates.

Similar to earlier studies (for example Khimitsa, 1968), four water masses are identified using a newly compiled hydrographic data set. Among them, the origin of RSW is well known. Hence, we will focus on identifying the origins of other the three water masses, the GASW, GAIW and GABW.

Being surface water, both seasonal and monthly variability was highest for the GASW. Though the core density is ~1024.10 kg m^{-3}, the lower limit of density varied from 1023.50 kg m^{-3} in winter to 1022.20 kg m^{-3} in summer due to the increase in temperature. The salinity of the core increased towards the west (Figs. 5 and 6). The θ-S-σ_θ structure of this water mass (core θ-S 26.0°C–36.0 psu and σ_θ 24.1) is similar to the salinity maximum D of Rochford (1964) and ASHSW described in Shenoi *et al*. (1993). The salinity maximum D of ASHSW forms in the surface of Arabian Sea and spreads along the σ_θ level 23.8 (θ-S range 24.0–26.5°C and 35.1–36.5 psu). The θ-S range of GASW is 21.0–32.0°C and 35.4–36.8 psu and core σ_θ is ~24.1 kg m^{-3}. However, in summer the temperature of this surface water increases to 31.5°C, while in winter it decreases to 26.0°C. The θ-S profiles (Antonov *et al*., 1998 and Boyer *et al*., 1998) from the western Arabian Sea (west of 60°E) show similar characteristics (figure
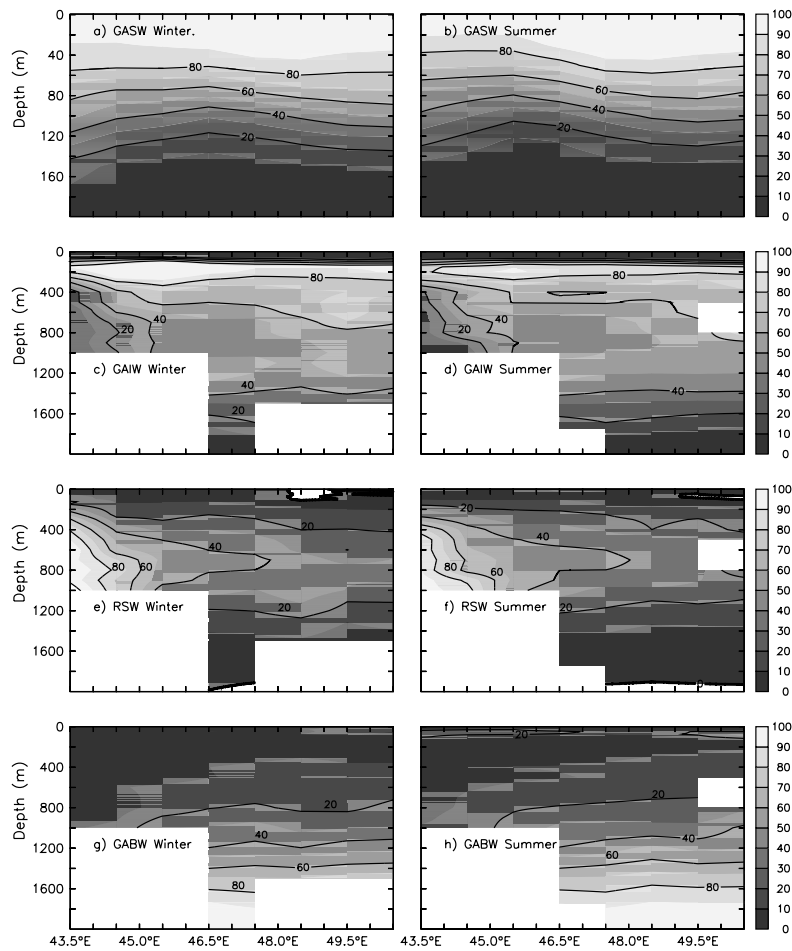

Fig. 10. Percentage composition of GA water. The water in the GA is presumed to be constituted due to the four water masses, namely, GASW, GAIW, RSW, and GABW.
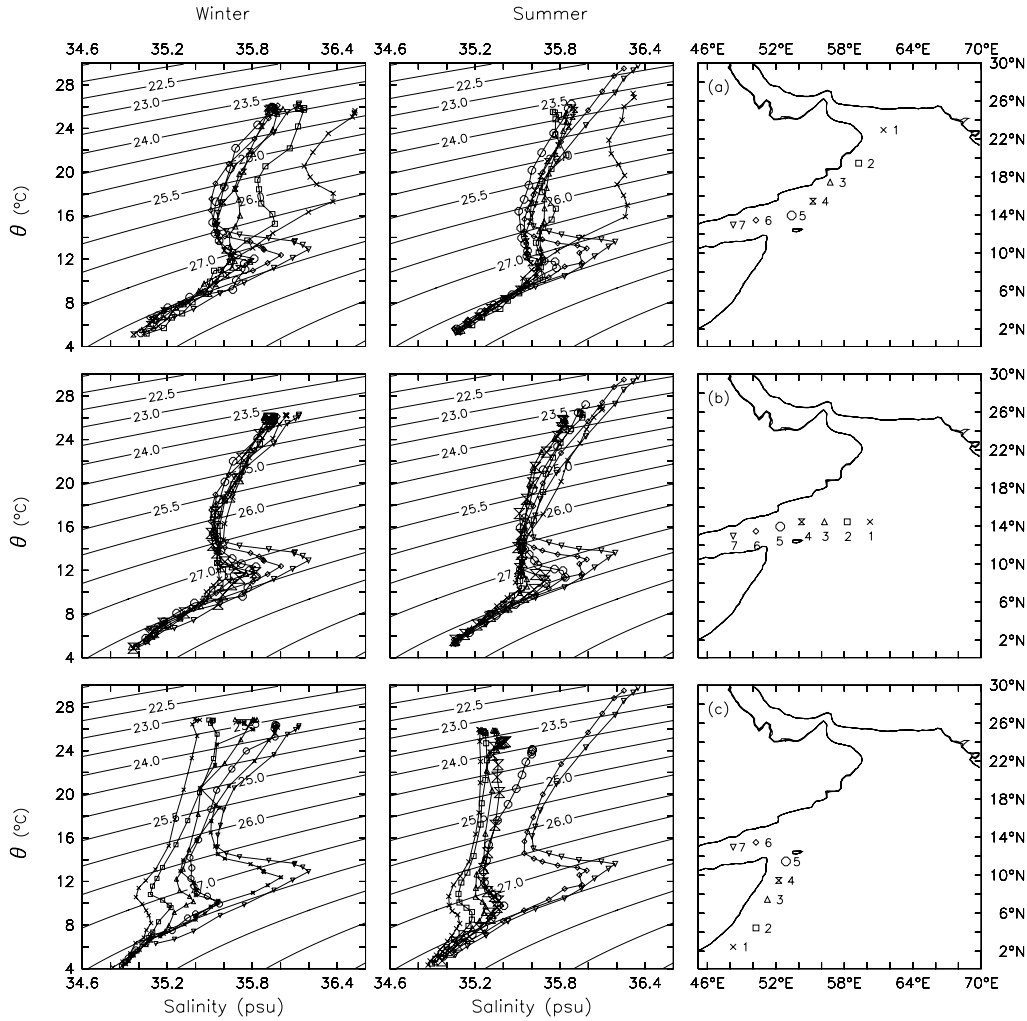
Fig. 11. θ-S curves at selected locations in the western Arabia Sea (see the corresponding map on the right side for the location of profiles) during winter and summer. Climatologies of Antonov *et al.* (1998) and Boyer *et al.* (1998) are used. The location of θ-S profiles were selected along three probable pathways of the water that might contribute to the GAIW. (a) from Persian Gulf to GA, (b) from the western Arabian sea to GA and (c) from the western equatorial Indian Ocean to GA.

not shown). The surface current is towards the west during winter and towards the east during summer (Khimitsa, 1968; Piechura and Sobaih, 1986; Al Saafani and Shenoi, 2006). Hence, during winter, a sizable amount of ASHSW will enter the GA from the east. Similarly, during summer, a sizable amount of surface water from the Red Sea will enter the GA from the west. In addition, during both seasons, some water will form locally due to precipitation and evaporation. Hence, it is possible that during winter the GASW forms as a mixture of locally formed water and ASHSW, while during summer it is a mixture of locally formed water and Red Sea surface water.

In the intermediate layers (200–300 m), the GAIW, appears as a minimum in the θ-S diagram at σ_θ level 26.5. Usually, a minimum occurs between two maxima and it

is unnecessary to trace its origin or determine the processes that actively depress the salinity. However, this particular minimum does not appear to be the typical minimum found between two maxima because (i) in the θ-S structure it appears as a distinct water mass (Fig. 3) and (ii) it is seen only at a particular σ_θ level and not spread over the entire water column between the two maxima. Hence it is necessary to identify the source of this minimum. Khimitsa (1968) suggested that the water in the intermediate level (150–200 m) enters the gulf as a strong jet between Cape Gvardafui and Socotra. Mohamed *et al.* (1996) identified the water between σ_θ levels 26.0 and 27.0 as a mixture of PGW, Arabian Sea Water and Timor Sea water.

To identify the pathways of GAIW, a series of θ-S

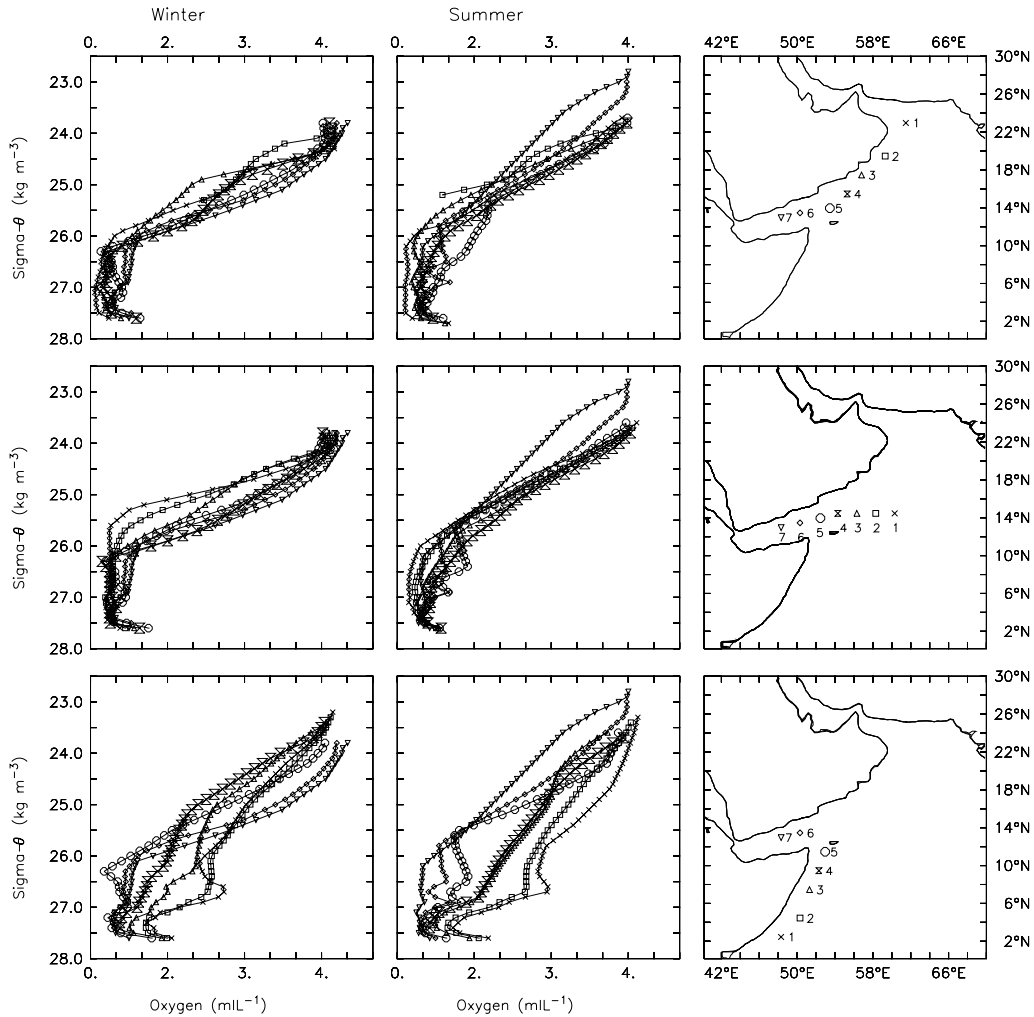Fig. 12. As Fig. 11, except that curves are for O_2 vs. σ_θ. This figure is also used to trace the pathway of GABW.

diagrams were constructed using data from Antonov *et al.* (1998) and Boyer *et al.* (1998) for selected locations along three paths: (i) from Gulf of Oman to GA (Fig. 11(a)); (ii) from the western Arabian Sea to GA (Fig. 11(b)); and (iii) from equator to GA (Fig. 11(c)). The θ-S profiles constructed along the path from Gulf of Oman to GA show maxima at $\sigma_\theta = 26.5$, corresponding to Persian Gulf Water (PGW), to station 3, which is situated outside the GA. From station 4 onwards, the station situated just outside the GA, the maximum is replaced by a minimum at $\sigma_\theta = 26.5$ and its salinity decreases further at station 5, the entrance to GA (Fig. 11(a)). The minimum is well marked at stations 6 and 7, inside the gulf. Thus, PGW cannot be the source of GAIW. The sections made normal to the coast of Oman (Morrison, 1997) also suggest very little flow of PGW towards south along the coast of Oman. Most of the PGW flows towards the east and later spreads towards south following the eastern boundary of

the Arabian Sea basin (Shenoi *et al.*, 1993).

The θ-S curves at locations along the paths from the western Arabian Sea (west of 60°E) to GA as well as that along the path from the equator to GA show the presence of salinity minima at around $\sigma_\theta = 26.5$ (Figs. 11(b) and (c)). Hence, it is likely that the GAIW enters the Gulf either from the south or the east. During summer, a well developed northward flow (Somali current) penetrates far deeper with velocities above 50 cm s^{-1} at 300 m depth; it transports about 37 ± 5 Sv of water off the coast of Somalia (Beal and Chereskin, 2003). Part of the Somali current system enters GA through the passage between Socotra and the Horn of Africa (Schott and McCreary, 2001). Fischer *et al.* (1996) estimated the total transport, west of Socotra, into the GA during summer as 13–14 Sv. Figures 5, 6 and 10 also indicate the east-to-west spread of GAIW. If the GAIW, which has a characteristic salinity minimum, enters the Gulf from the western Arabian

Sea, especially through the Socotra passage, then what is the source of low salinity water in the western Arabian Sea?

Three sources have been identified for the low salinity water in the western Arabian Sea, the Somali basin. First, the low salinity water brought into the Somali basin by the northern branch of the South Equatorial Current (SEC) (Swallow *et al.*, 1983); this brings the water from the eastern equatorial Indian Ocean. Warren *et al.* (1966) recognized the Bay of Bengal as a likely source of fresh water for the Somali basin. Morrison (1997) reported the presence of low saline Indian Central Water in the western Arabian Sea at σ_θ = 26.6. However, Wyrtki (1971) suggested that the water of SEC in the lower thermocline (18.0–19.0°C) originates near the Indonesian archipelago and not from the Bay of Bengal. This water flows at the density surface σ_θ = 25.0.

The second possibility is the low salinity Subtropical Subsurface Water (SSW), which originates at the Subtropical Convergence in the southern hemisphere near 40°S (Quadfasel and Schott, 1982). Warren *et al.* (1966) and Wyrtki (1971) showed that this water penetrates as far as 10°N off East Africa and is partially responsible for the low salinity in the intermediate layer of the northern Somali basin. In the Somali basin, in the density range from σ_θ = 26.5 to 27.0, its core layer lies between 300 and 400 m. The temperature varies between 8.0 and 15.0°C and salinity between 34.8 and 35.5 psu (Quadfasel and Schott, 1982). This description of SSW matches well with the salinity minimum associated with GAIW. The salinity minimum that lies on the σ_θ level 26.5 in the GA has a potential temperature range between 11.0 and 18.0°C and salinity between 35.0 and 36.4 psu; its core layer lies between 200 and 300 m. The corresponding thermohaline index (Table 2) was σ_θ = 14.5°C and S = 35.25 psu.

The third possibility is the Antarctic Intermediate Water (AIW), which forms at the Antarctic Convergence Zone at around 40–50°S, sinks and flows north. This water is characterized by low salinity (<34.3 psu) and high oxygen content (>5.0 ml L^{-1}); at its source the core layer σ_θ is 27.4. Wyrtki (1971) reported its existence at 5°S and Quadfasel and Schott (1982) at 4°S at the depth rage 700–800 m. Tchernia (1980) suggested that AIW could extend to the extreme northwest Indian Ocean at the Gulf of Aden and Gulf of Oman, where it rises up to depths as shallow as 200–300 m in order to override the relatively saline water spreading southwestward from the Arabian Sea. Hence, it is possible that both SSW and AIW contribute to the existence of the salinity minimum in the GA at intermediate levels.

The Socotra passage seems to be the main connection between GA and Somali Basin. The passage also acts as the pathway for the southward migration of RSW. A southward under-current below the northward Somali current in the latitude band 8–12°N (Quadfasel and Schott, 1983; Schott and Fischer, 2000) transports the RSW southward at depths ~600–1000 m.

The GABW identifiable in the σ_θ range 27.5 to 27.8 occupies about 35% of the total volume of GA. Khimitsa (1968) identified this water with the water originating from the Southern Ocean. Since there is no production of bottom water in the Arabian basin (Quadfasel *et al.*, 1997) it is necessary to transport the bottom water from elsewhere. Johnson *et al.* (1998) showed that approximately 1–1.7 Sv of Circumpolar Deep Water (CDW) enters the Somali basin through Aminrante Passage at 8°S. The potential density of this water is much higher (σ_θ > 28.5) than the GABW, and its representative θ-S characteristic is 1.0–1.1°C and 34.72–34.75 psu. Hence it is not possible to identify the GABW with CDW. Another possibility is the water of southern origin, as noted in the θ-S and θ-O$_2$ curves of Johnson *et al.* (1998). This water having $\theta \sim$ 3°C has low salinity (34.70–34.72) and higher oxygen content (see figure 3 of Johnson *et al.*, 1998). Although Johnson *et al.* (1998) do not specify the southern source of this water it is possible that the AIW could be one among them because that also is characterized by low salinity and high oxygen content. From Figs. 11 and 12 it appears that this water of southern origin spreads further north into the GA (between the σ_θ levels 27.5 and 27.8). The θ-S (Fig. 11) and the σ_θ-O$_2$ curves (Fig. 12) show lower salinity and higher oxygen for this water (~2.0 ml L^{-1} near the equator). The water of southern origin that enters the GA from the south, through the Somali Basin, ultimately mixes with the high saline RSW to produce the GABW with salinity more than 34.80 psu. The mixing of warm RSW with cooler water from the south leaves a wide range of potential temperature (2–11°C). The percentage compositions estimated based on the mixing theory of water masses (Fig. 10) suggest the presence of ~10–20% RSW in the GABW. Fedorov and Meshchanov (1988) and Mecking and Warner (1999) have shown that some RSW remains relatively undiluted (at σ_θ > 27.5) as it flows out of the Red Sea and descends in the western GA. Hence, the bottom water in the western most GA could be the RSW itself.

References

Al Saafani, M. A. and S. S. C. Shenoi (2004): Seasonal cycle of hydrography in the Bab el Mandab region, southern Red Sea. *Proceedings Earth and Planetary Sciences*. **113**(3), 269–280.

Al Saafani, M. A. and S. S. C. Shenoi (2006): Seasonal and interannual variability of eddy field and surface circulation in the Gulf of Aden. *Presented at "15 years of Progress in Radar Altimetry Symposium" 13–18 March 2006*, Venice, Italy.

Antonov, J. I., S. Levitus, T. P. Boyer, M. E. Conkright, T. O'Brien, C. Stephens and B. Trotsenko (1998): World Ocean Atlas 1998 Vol. 3. Temperature of the Indian Ocean. *NOAA Atlas NESDIS 29*, U.S. Government Printing Office, Washington, D.C.

Baars, M. A. (1994): Monsoons and pelagic systems. *Cruise Reports Netherlands Indian Ocean Programme, Vol. 1 (National Museum of Natural History, Leiden)*, 143 pp.

Beal, L. M. and T. K. Chereskin (2003): The volume transport of the Somali Current during the 1995 southwest monsoon. *Deep-Sea Res. II*, **50**, 2077–2090.

Bower, A. S., D. H. Hunt and J. F. Price (2000): Character and dynamics of the Red Sea and Persian Gulf outflows. *J. Geophys. Res.*, **105**(C3), 6387–6414.

Bower, A. S., W. E. Johns, D. M. Fratantoni and H. Peters (2005): Equilibration and circulation of Red Sea Outflow Water in the western Gulf of Aden. *J. Phys. Oceanogr.* (in press).

Boyer, T. P. and S. Levitus (1994): Quality control and processing of historical temperature, salinity and oxygen data. *NOAA Technical Report NESDIS 81*, 65 pp.

Boyer, T. P., S. Levitus, J. I. Antonov, M. E. Conkright, T. O'Brien, C. Stephens and B. Trotsenko (1998): World Ocean Atlas 1998 Vol. 6. Salinity of the Indian Ocean. *NOAA Atlas NESDIS 32*, U.S. Government Printing Office, Washington, D.C.

Boyer, T. P., C. Stephens, J. I. Antonov, M. E. Conkright, R. A. Locarnini, T. D. O'Brien and H. E. Garcia, (2002): World Ocean Atlas 2001 Vol. 2. Salinity. *NOAA Atlas NESDIS 50*, ed. by S. Levitus, U.S. Government Printing Office, Washington, D.C., 176 pp.

Fedorov, K. N. and S. L. Meshchanov (1988): Structure and propagation of Red Sea waters in the Gulf of Aden. *Oceanology*, **28**(3), 279–284.

Fischer, J., F. Schott and L. Stramma (1996): Currents and transports of the Great Whirl-Socotra Gyre system during the summer monsoon, August 1993. *J. Geophys. Res.*, **101**, 3573–3587.

Johnson, G. C., D. L. Musgrave, B. A. Warren, A. Ffield and D. B. Olson (1998): Flow of bottom and deep water in the amirante passage and Mascarene Basin. *J. Geophys. Res.*, **103**(C13), 30973–30984.

Khimitsa, V. A. (1968): The hydrological structure of the waters of the Gulf of Aden. *Oceanology*, **8**, 318–322.

Maillard, C. and G. Soliman (1986): Hydrography of the Red Sea and exchanges with the Indian Ocean in summer. *Oceanol. Acta*, **9**, 249–269.

Mecking, S. and M. J. Warner (1999): Ventilation of Red Sea water with respect to Chloro norocarbons. *J. Geophys. Res.*, **104**, 11087–11097.

Mohamed, E. E. E., S. H. Sharaf El-Din and A. A. H. El-Gindy (1996): Dynamic and hydrographic structure in the Red Sea and Gulf of Aden. p. 78–101. In *Present and Future of Oceanographic Programs in Developing Countries, Vienna and Honolulu*, Durvasula,-S.V., Visakhapatnam-India Andhra-University 1996 No. 3.

Mohammed, E. E. E. (1997): On the variability, potential energy, potential temperature, salinity and currents in NW Indian Ocean and Gulf of Aden. *JKAU. Mar. Sci.*, **8**, 47–65.

Montgomery, R. B. (1958): Water characteristics of Atlantic Ocean and of world. *Deep-Sea Res.*, **5**, 134–148.

Morrison, J. M. (1997): Inter-monsoonal changes in the T-S properties of the near-surface waters of the northern Arabian Sea. *Geophys. Res. Lett.*, **24**(21), 2553–2556.

Murray, S. P. and W. Johns (1997): Direct observations of seasonal exchange through the Bab el Mandab Strait. *Geophys. Res. Lett.*, **24**, 2557–2560.

Nasser, G. A. (1992): Seasonal changes in the water characteristics of upper 1000 m in the northern Gulf of Aden. In *Scientific Investigation of the Gulf of Aden. Vol. II*, Mar. Sci. and Resources Res. Center, Aden, Yemen.

Ozgokman, T. M., W. E. Johns, H. Peters and S. Matt (2003): Turbulent mixing in the Red Sea outflow plume from a high-resolution nonhydrostatic model. *J. Phys. Oceanogr.*, **33**, 1846–1869.

Peter, H. and W. E. Johns (2005): Mixing and entrainment in the Red Sea outflow plume. II. Turbulence characteristics. *J. Phys. Oceanogr.*, **35**(5), 584–600.

Peter, H., W. E. Johns, E. S. Bower and D. M. Fratantoni (2005): Mixing and entrainment in the Red Sea outflow plume. I. Plume structure. *J. Phys. Oceanogr.*, **35**(5), 569–583.

Piechura, J. and O. A. G. Sobaih (1986): Oceanographic conditions of the Gulf of Aden. *Sci. Invest. Gulf Aden, Series A: Oceanography*, No. 2.

Quadfasel, D. and F. Schott (1982): Water-mass distribution at intermediate layers off the Somali Coast during the onset of the southwest monsoon 1979. *J. Phys. Oceanogr.*, **12**, 1358–1372.

Quadfasel, D. and F. Schott (1983): Southward subsurface flow below the Somali Current. *J. Geophys. Res.*, **88**, 5973–5979.

Quadfasel, D., J. Fischer, F. Schott and L. Stramma (1997): Deep water exchange through the Owen Fracture Zone in the Arabian Sea. *Geophys. Res. Lett.*, **24**, 2805–2808.

Rochford, D. J. (1964): Salinity maxima in the upper 1000 meters of the north Indian Ocean. *Aust. J. Mar. Freshw. Res.*, **15**, 1–24.

Schott, F. and J. Fischer (2000): Winter monsoon circulation of the northern Arabian Sea and Somali Current. *J. Geophys. Res.*, **105**, 6359–6376.

Schott, F. A. and J. P. McCreary (2001): The monsoon circulation of the Indian Ocean. *Prog. Oceanogr.*, **51**, 1–123.

Shenoi, S. S. C., R. Shetye, A. D. Gouveia and G. S. Micheal (1993): Salinity extrema in the Arabian Sea. p. 37–49. In *Monsoon Biogeochemistry*, ed. by V. Ittickkot and R. R. Nair, Mitt Geol. Palaont. Inst. Univ. Hamburg, Humburg, Germany.

Stephens, C., J. I. Antonov, T. P. Boyer, M. E. Conkright, R. A. Locarnini, T. D. O'Brien and H. E. Garcia, (2002): World Ocean Atlas 2001 Vol. 1. Temperature. *NOAA Atlas NESDIS 49*, ed. by S. Levitus, U.S. Government Printing Office, Washington, D.C., 176 pp.

Stirn, J., R. Edwards, J. Pichura, M. Savich, M. Ghaddaf, M. Fadel, F. Mutlag, O. A. G. Sobaif, A. Al-Sayed, A. Shaer and Z. Zubairi (1985): Oceanographic conditions, pelagic productivity and living resources in the Gulf of Aden. *IOC/ UNESCO Workshop on Regional Co-operation in Marine Science in the Central Indian Ocean and Adjacent Seas and Gulfs*, Colombo, Report No. 37, 225 pp.

Swallow, J. C., R. L. Molinari, J. G. Bruce, O. B. Brown and R. H. Evans (1983): Development of near-surface flow pattern and water mass distribution in the Somali Basin in response to the southwest monsoon of 1979. *J. Phys. Oceanogr.*, **13**, 1398–1415.

Tchernia, P. (1980): *Descriptive Regional Oceanography*. (Pergamon Marine Series, 3), Pergamon, Oxford, U.K., XVIII + 253 pp.

Tomczak, M., Jr. (1981a): Non-isopycnal mixing in the frontal zone of South and North Atlantic Central Water off North-West Africa. *Prog. Oceanogr.*, **10**(3), 147–171.

Tomczak, M., Jr. (1981b): A multi-parameter extension of temperature/salinity diagram techniques for the analysis of non-isopycnal mixing. *Prog. Oceanogr.*, **10**(3), 173–192.

Warren, B. A., H. Stommel and J. C. Swallow (1966): Water masses and pattern of flow in the Somali Basin during the southwest monsoon of 1964. *Deep-Sea Res.*, **5**, 108–109.

Wyrtki, K. (1971): *Oceanographic Atlas of the International Indian Ocean Expedition*. 521 + xi pp., Super. of Doc., U.S. Government Printing Office, Washington, D.C.